

An experimental study of the Leidenfrost evaporation characteristics of emulsified liquid droplets

C. T. AVEDISIAN and M. FATEHI

Sibley School of Mechanical and Aerospace Engineering, Cornell University, Ithaca, NY 14853, U.S.A.

(Received 6 October 1986 and in final form 20 November 1987)

Abstract—Experimental observations of the evaporation characteristics of water-in-fuel emulsion droplets in film boiling on a hot horizontal surface are reported. Detailed measurements of the temporal variation of equivalent droplet diameter for water-in-heptane and water-in-decane emulsions are made at surface temperatures of 565, 620 and 680 K. Experiments are performed at atmospheric pressure and initial water volume concentrations of 10, 20, 35 and 50%. More qualitative characteristics are observed for emulsions of water in octane, nonane and dodecane. It is found that water/heptane and water/decane emulsions exhibit preferential vaporization such that either the water or hydrocarbon evaporate first (for decane or heptane emulsions, respectively). This result is revealed by an apparent discontinuity in the evolution of equivalent droplet diameter and is explained on the basis of a simple distillation limit model for evaporation. Results also show that the droplet evaporation rate decreases, and the total droplet evaporation time increases, with increasing water content. The initially opaque colored droplets appear to clear up during vaporization for several of the emulsions tested. Coalescence of the internal phase for water/octane and water/dodecane emulsions is also observed. Of the emulsions tested, only the water/heptane emulsions exhibit a disruptive characteristic at the end of the evaporation process.

1. INTRODUCTION

THE USE of water as an additive to hydrocarbon fuels, thus forming an emulsion, has been proposed to reduce the fire vulnerability of propulsion devices [1], to improve combustion efficiency [2], and to mitigate the formation of oxides of nitrogen during combustion [3]. In most applications, the emulsion will be used in the form of a spray, the component droplets of which could impact the confinement boundary of the spray (which could be an impermeable surface, a porous surface, or another liquid).

The present work addresses the problem of droplet/solid surface interactions from the perspective of a single isolated emulsified liquid droplet softly deposited and subsequently evaporating at a horizontal impermeable surface above the Leidenfrost temperature of the emulsion. The purpose was to study the characteristics and mechanisms governing the evaporation of emulsified liquid droplets at a hot surface. In the course of this work, information pertinent to the general evaporative characteristics of emulsified liquids was also obtained. The effects of water concentration in water/heptane and water/decane emulsions on the evaporation rate and total evaporation time at atmospheric pressure are reported. Heptane was chosen for the continuous phase to simulate a fuel which has a boiling point close to that of water, while decane was chosen to model a volatile/non-volatile system. The boiling points of both heptane and decane are lower than the

superheat limits of their respective emulsions with water at atmospheric pressure so that internal homogeneous nucleation, and micro-explosions should not be expected. This latter phenomenon was not of direct interest in this work.

Most previous experimental work on film evaporation of droplets at hot surfaces have employed a variety of pure liquids, mixtures, solid suspensions and surface materials (e.g. see refs. [4–10]). Two studies are known which specifically deal with emulsion droplets at surfaces [11, 12].

Sheffield *et al.* [11] focused attention on the micro-explosion characteristics of emulsions at hot surfaces. They observed that droplets in film evaporation often exploded violently when water was mixed with several high boiling point hydrocarbons (e.g. hexadecane).

Cho [12] studied the ignition and micro-explosion characteristics of water-in-oil emulsions. He observed that at pressures above 3 atm no micro-explosions occurred even for emulsions of water with hexadecane. It was further noted that at subatmospheric pressures, micro-explosion was suppressed. In addition Law *et al.* [13] also mentioned some preliminary qualitative observations of emulsified droplets evaporating at hot surfaces, noting several characteristics reported in greater detail here.

Specific objectives of the present experiments were to:

(a) determine the variation of the effective diameter of an emulsion droplet as a function of time;

NOMENCLATURE

C_p	average vapor specific heat in levitation film	y	non-dimensional coordinate measured from the center of the levitation film.
D	binary gas diffusion coefficient	Greek symbols	
d_e	equivalent droplet diameter	δ	levitation height
d_0	initial droplet diameter	ε_i	fractional evaporation rate of component i
f_1	volume truncation factor	μ_g	average vapor viscosity in levitation film
f_2	surface area truncation factor	ρ_g	total gas density
g	gravitational constant	ρ_i	vapor density
h_m	mass transfer coefficient	ρ_1	volume fraction average density of emulsion
K	evaporation 'constant'	τ	non-dimensional time
k_g	average vapor thermal conductivity in levitation film	ϕ	non-dimensional mass concentration
L	latent heat of vaporization	Φ	initial water volume fraction of emulsion.
m	mass evaporation rate per unit area, $\Sigma_i m_i$	Subscripts	
P_0	total pressure in levitation film	i	component i (1 (water), 2 (hydrocarbon))
P_{ic}	saturation pressure of component i	ib	component i in the 'bulk' of the levitation film
Sh	Sherwood number, $h_m \delta / D$	is	component i at droplet surface
t	time	m	average value
T_s	steady-state droplet temperature	s	droplet surface.
T_p	hot surface temperature		
ΔT	$T_p - T_s$		
V_0	initial droplet volume		
\bar{V}	non-dimensional droplet volume		

(b) determine the variation of total evaporation time as a function of initial volume fraction of water for emulsions;

(c) photographically document the evaporative behavior of the droplets.

Information on the evolution of effective diameter in particular will provide insight into possible preferential evaporation mechanisms. Conditions of the experiments were the following:

pressure: atmospheric;

surface temperatures: 565, 620 and 680 K;

emulsion components: heptane and decane emulsions containing water;

initial water volume percentage: 10, 20, 35, 50%;

test surface material: polished stainless steel.

In addition, more qualitative evaporative characteristics are reported for emulsions of water with octane, nonane and dodecane.

2. APPARATUS AND EMULSION PREPARATION

2.1. Description of the apparatus

The experimental method consisted of placing a droplet of known volume (approximately 12 μl in our experiments) on a hot surface and then recording its evaporative history by photographic means. Figure 1 is a schematic diagram of the apparatus. Principle

components are (1) a heating unit (a cylindrical copper billet 6.35 cm in diameter and 80 cm long around which two 450 W band heaters are fastened), (2) a removable polished test surface (stainless steel) 6.35 cm in diameter, 1.9 cm thick and with a 1° conical indentation machined in the center of the upper face, (3) a droplet injector (syringe), (4) 35 mm camera system and associated close-up accessories for high precision droplet diameter measurements, and (5) a video-optical system for rapid measurements of total droplet evaporation times.

Droplets were deposited on the test surface using a 50 μl syringe (Gastight # 1705) fitted with a flat-tipped needle (0.91 mm o.d.). The needle tip was positioned about 1 cm above the hot plate and the plunger slowly depressed until a droplet detached from the needle by its own weight. Droplet volumes were calibrated by measuring the total volume of 100 droplets deposited in a graduated cylinder.

The test surface was prepared by polishing it with # 5 Emery paper and Wenol Plus K compound, and then washing with acetone. It was necessary to polish the surface in this manner each time for each droplet tested because a residue of surfactants was deposited on the surface after evaporation of a droplet.

The test surface temperature was determined by extrapolating the measurements of four chromel/alumel 1.6 mm diameter thermocouples inserted within the surface at vertical spacings of 10 mm. The extrapolated surface temperatures were found to be

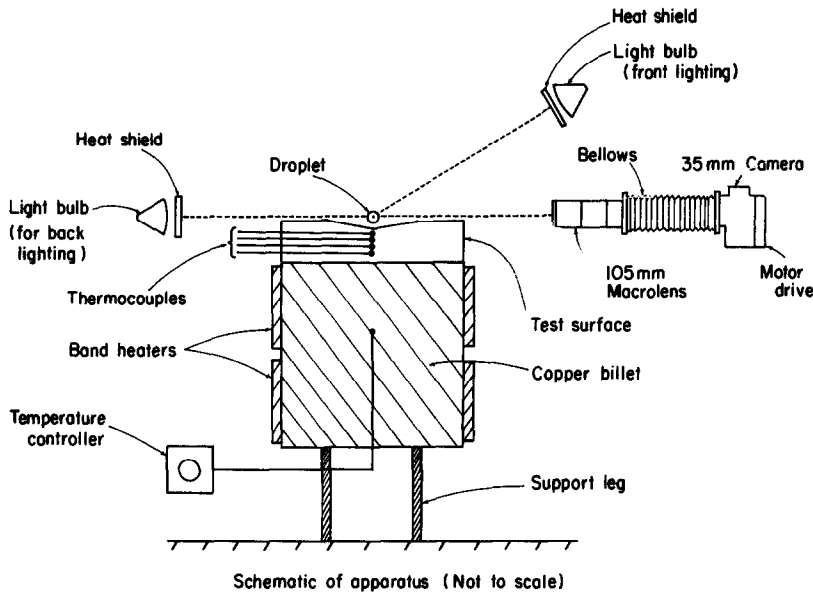


FIG. 1. Schematic diagram of the apparatus.

within 1 K of the temperature measured by the uppermost thermocouple (located 1.5 mm below the center of the surface). Temperatures were continuously monitored by an Omega temperature logger (model OM202), and the surface temperature was regulated by an Omega temperature controller (model E924).

The evolution of droplet size was measured from high contrast droplet images obtained from 35 mm photographic sequences. A 35 mm Nikon F3 camera fitted with a 105 mm macro lens and an extension bellows (model PB6) was used to take successive pictures of a droplet during its evaporation. The film was advanced by a Nikon motor-drive unit (model MD4) connected to a pulse generator (HP model 3311A). Framing rates of 1 and 2 frames s^{-1} were used. Back lighting was provided by a single GE FHX 25 W 13 V bulb equipped with heat absorbing glass to prevent extraneous heating of the droplet by the light source. The light bulb was positioned 8 cm away from the center of the surface and 1 cm above it. The camera lens was positioned on the opposite side 7 cm away from the center of the plate and 1 cm above it, thus providing a nearly planar view of the drop. The bellows was extended 18 cm. Care was taken to align the center of the light bulb with the center of the plate and the center of the camera lens. A shutter speed of 2000 s^{-1} , an *f*/stop of 32, and Kodak black and white film with ASA125 were used.

Additional black and white photographs using direct *front* lighting were taken to observe qualitative textural and opacity changes of the droplets during their evaporation. For this purpose two 75 W light bulbs were placed at 45° angles, 60 cm high with respect to the test surface, and 30 cm away from the plate center.

Droplet dimensions were obtained by first making magnified photocopies of the 35 mm negatives (using a microfilm reader) and then obtaining the droplet dimensions by using a planimeter to trace around the droplet's image. An equivalent diameter, d_e , was defined from these measurements as

$$d_e = 2(A_{\text{meas}}/\pi)^{1/2} \quad (1)$$

where A_{meas} is the scaled projected cross-sectional area of the droplet. This procedure assumes the droplet is a volume of revolution of the projected area; further discussion of this point is given in Section 3.1.

2.2. Emulsion preparation

The emulsions were stabilized with 3% by volume of a surfactant mixture and prepared in small samples of 103 ml. The hydrocarbons were first mixed with the surfactant mixture and then water was added, drop by drop. The emulsions were continuously agitated by a 20 000 Hz Sonic Dismembrator (Fisher model No. 300) for 5 min during this mixing. The surfactants consisted of Span 80 and Tween 80 mixtures as suggested by Wang [14]. They were obtained from Atlas Chemical Co. The hydrocarbons were 99.6% pure, obtained from Humphrey Chemical Co. and used directly as received. The water was singly distilled.

The emulsion samples were placed in an ice bath during exposure to the ultrasonic transducer to prevent them from being heated during preparation with a possible degradation of stability. The samples were continuously agitated in the ice bath during testing. Samples were withdrawn from the center of the mixing beaker. All emulsions initially had a creamy white

appearance and were stable against visible separation at room temperature for about 1 day.

3. RESULTS AND DISCUSSIONS

3.1. Temporal variation of droplet diameter

Figures 2–8 show the variation of equivalent droplet diameter, normalized by the indicated initial effective diameter (d_0), with time for various water/heptane and water/decane emulsion. The lines through the data are curves of best fit to enhance the variation. The slopes of these lines are a measure of the so-called ‘evaporation constant’, defined here as

$$d_c^n = d_0^n - Kt \quad (2)$$

where we take $n = 1$; a theoretical value for a Leidenfrost droplet is $n = 1.25$ [15].

Water/decane emulsions containing 10, 20 and 35% water appeared to exhibit a preferential vaporization of water as revealed by an abrupt change in K (for most of the emulsions tested) sometime during evaporation as shown in Figs. 2–4. During an early period and at low plate temperatures, water apparently dominates evaporation in that $K \rightarrow K_{\text{water}}$. At later times the influence of water is reduced and the evaporation constant approaches that of pure decane, $K \rightarrow K_{\text{decane}}$,

as evidenced by comparing the slopes of the lines drawn through the data with the evaporation constants for the decane ($\Phi = 0$) and water ($\Phi = 1$) data. This change in K during evaporation is more clearly illustrated in Fig. 5 for a 35% water/decane emulsion with surface temperature as the parameter. A similar change in the evaporation constant has been previously observed by Law *et al.* [13] for a water/octane emulsion droplet containing 10% water and burning in an unbounded atmosphere while suspended from a fiber. With increasing water content ($\approx 50\%$) evaporation was found to be less dominated by water during the early period of evaporation and the evaporation constant was in the range of $K_{\text{water}} < K < K_{\text{decane}}$. This effect may be due to the possibility that water will participate in the evaporation process for a longer time than for lower concentrations. Such preferential evaporation has also been observed during evaporation of acoustically levitated butanol/water and undecane/butanol mixtures under certain conditions [16].

Water/heptane emulsion droplets also exhibited a preferential vaporization as shown in Figs. 6–8 for surface temperatures of 565, 620 and 680 K, respectively. Now, however, it was found that $K \rightarrow K_{\text{heptane}}$ during the early stages of evaporation. This difference

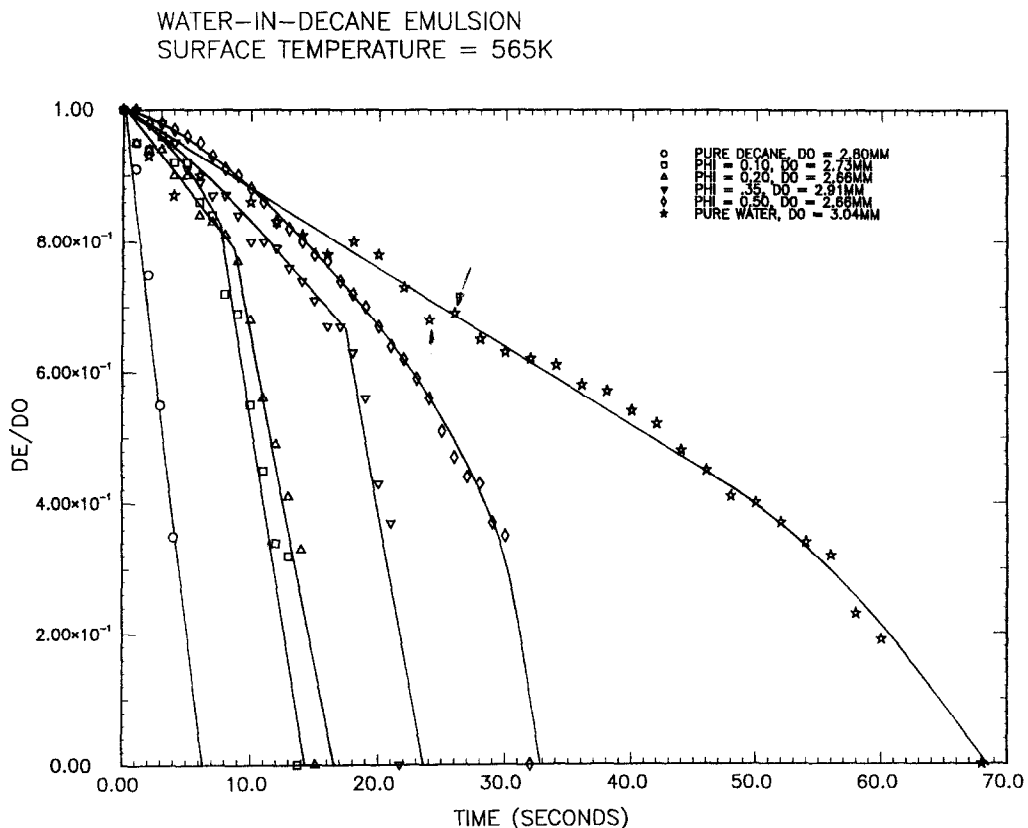


FIG. 2. Measured evolution of droplet diameter for various water/decane emulsion droplets at $T_p = 565$ K. Lines through data are curves of best fit.

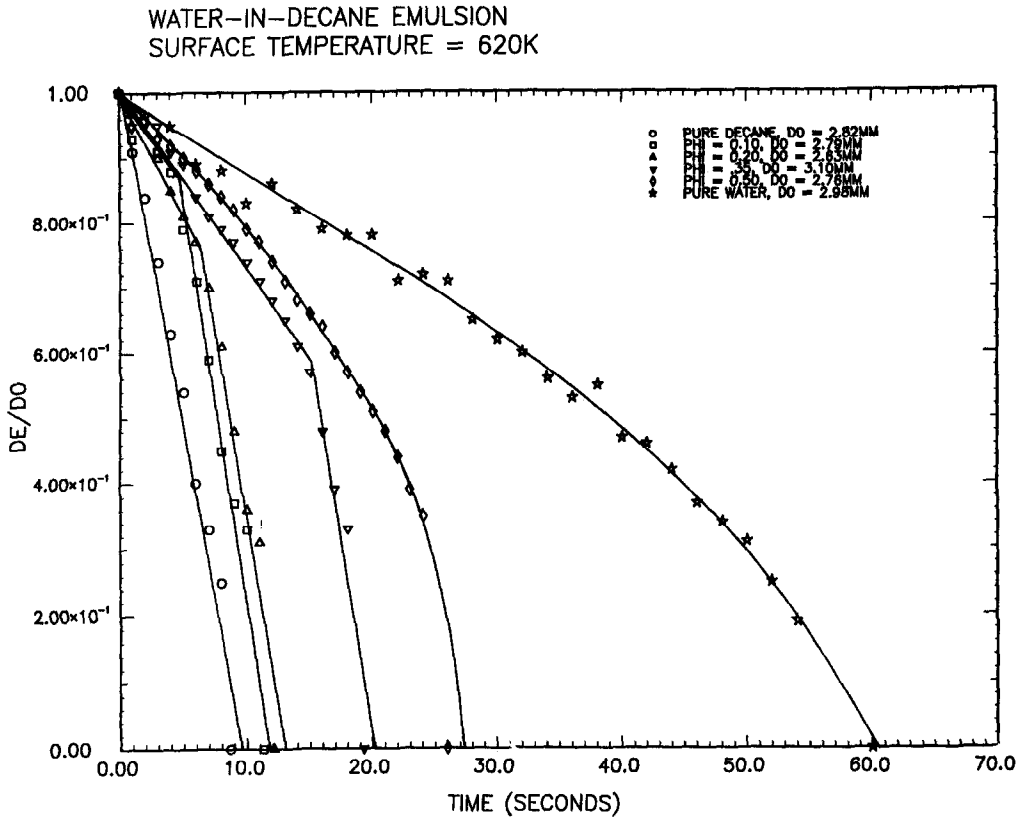


FIG. 3. Measured evolution of droplet diameter for various water/decane emulsion droplets at $T_p = 620$ K.

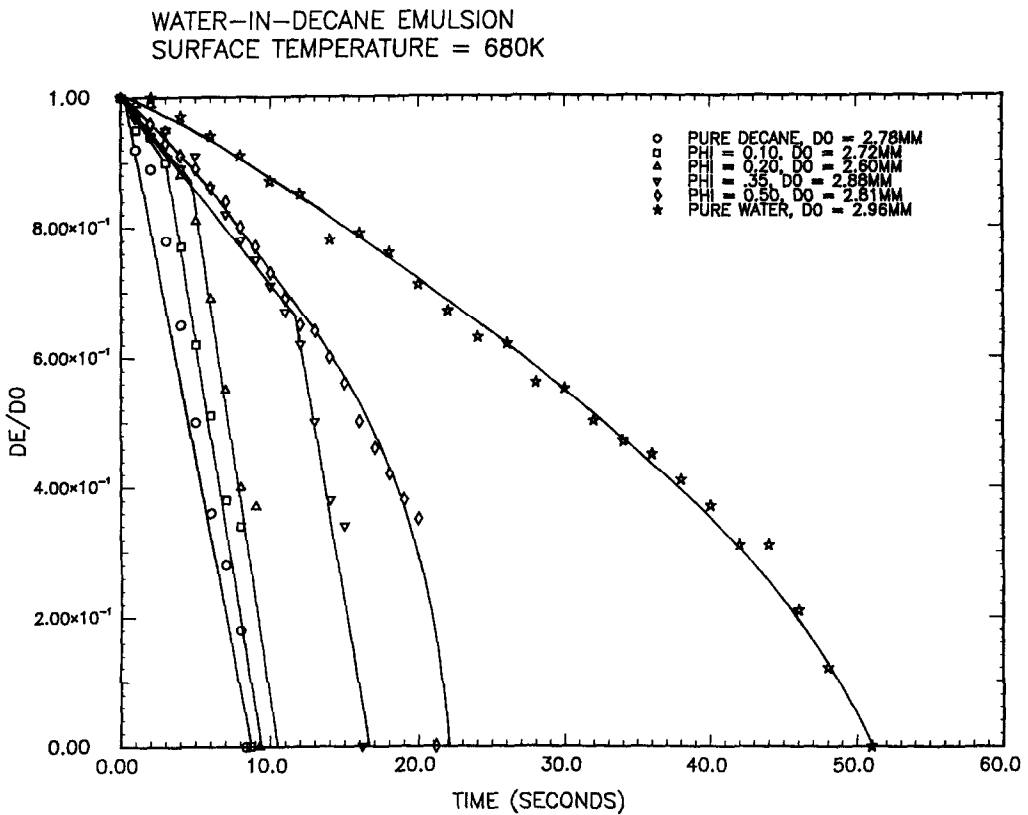


FIG. 4. Measured evolution of diameter for various water/decane emulsion droplets at $T_p = 680$ K.

35% WATER-IN-DECANE EMULSION AT SURFACE TEMPERATURES OF 565K, 620K, AND 680K

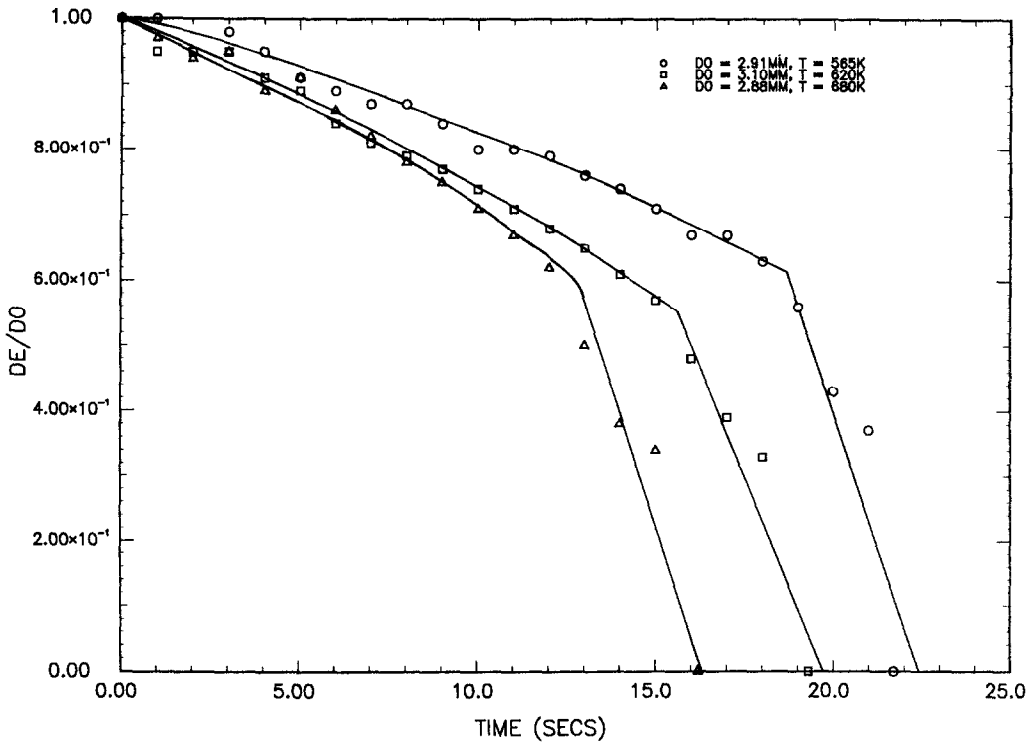


FIG. 5. Evolution of diameter for a 35% water-in-decane emulsion droplet at three surface temperatures.

WATER-IN-HEPTANE EMULSION
SURFACE TEMPERATURE = 565K

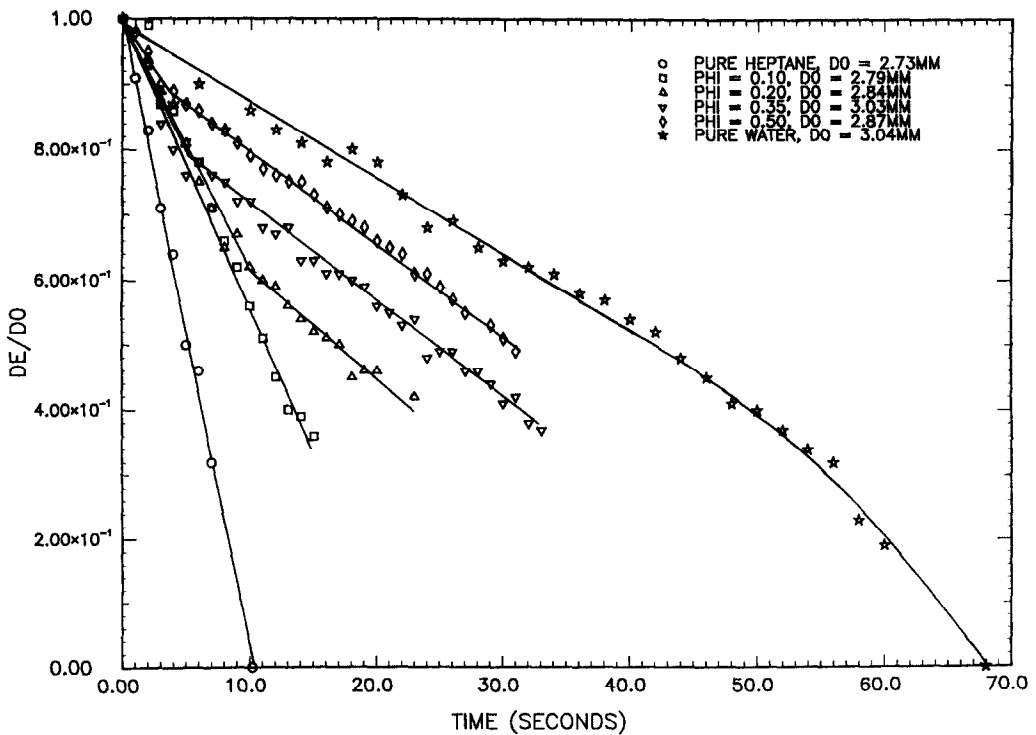


FIG. 6. Evolution of droplet diameter for several water/heptane emulsions at $T_p = 565$ K. Line through data is a curve of best fit.

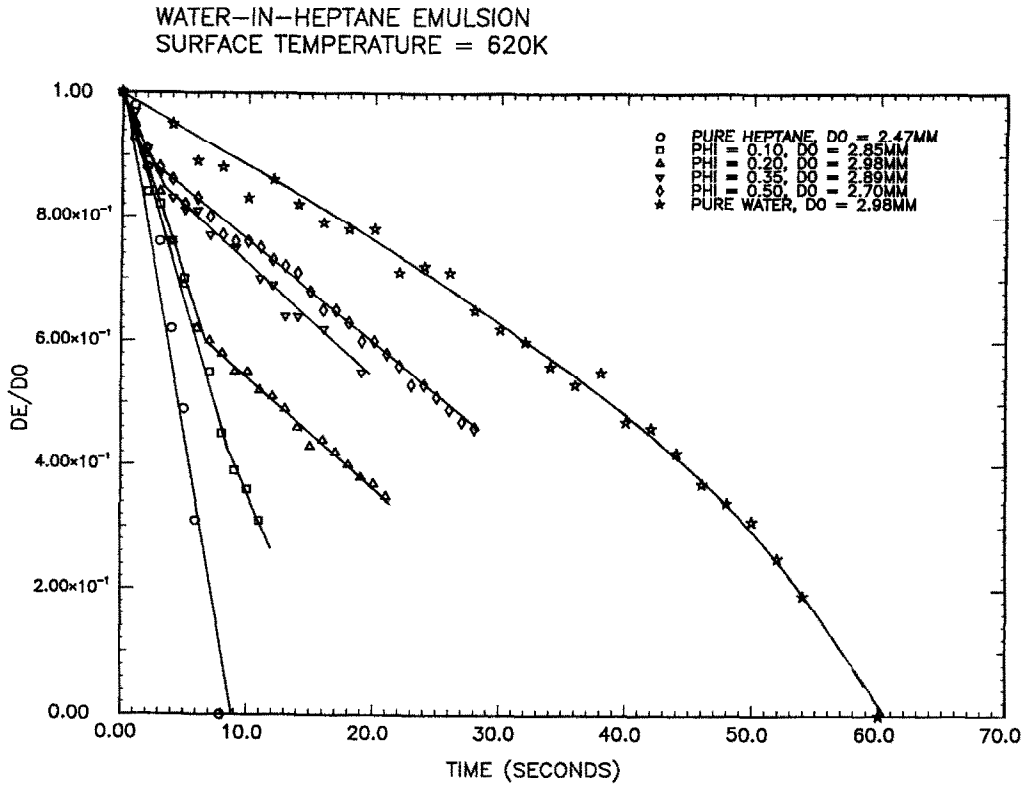


FIG. 7. Evolution of droplet diameter for several water/heptane emulsions at $T_p = 620$ K.

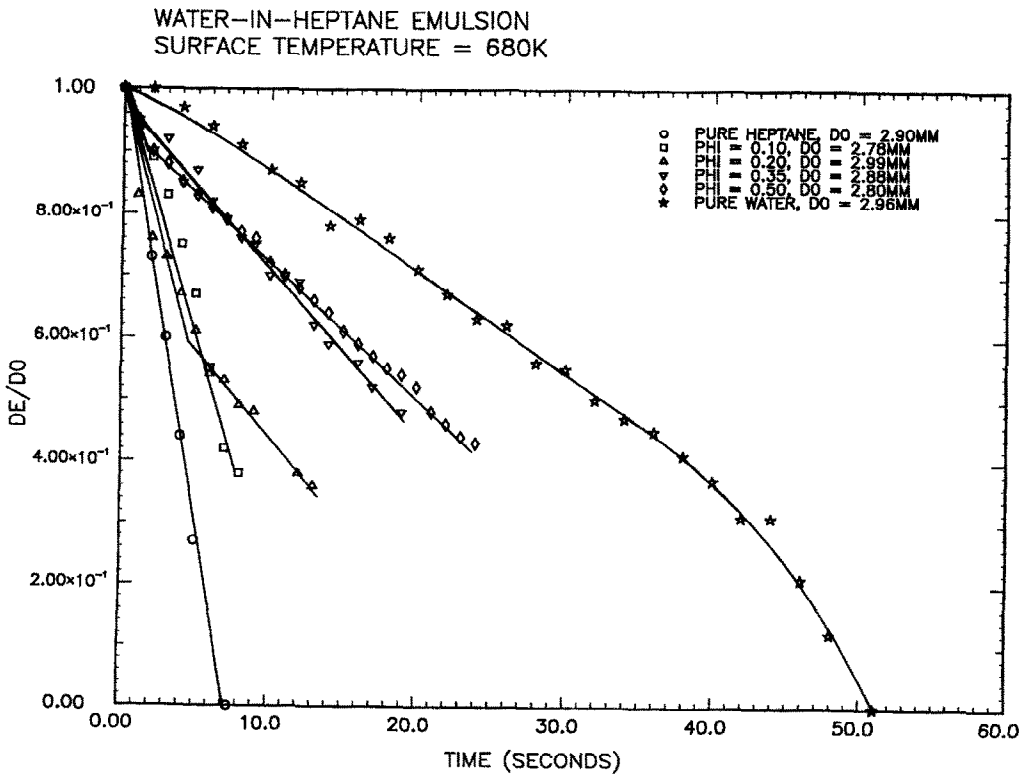


FIG. 8. Evolution of droplet diameter for several water/heptane emulsion droplets at $T_p = 680$ K.

in preferential evaporation between emulsions of heptane and decane with water is more clearly illustrated in Fig. 9. Here, the variation of normalized equivalent diameter with time for emulsions containing an initial water content of 20% is illustrated at a single surface temperature of 565 K. For water/heptane emulsions, heptane appeared to vaporize first (i.e. $K \approx K_{\text{heptane}}$ initially). At later times, water controlled evaporation. The opposite was true for decane emulsions. For low water concentrations ($\leq 10\%$ in Figs. 6–8), no change in the evaporation constant could be observed with time, the reason being that water vaporized over a period which was not detectable on the scale of Figs. 6–8.

An explanation for preferential vaporization of emulsion components in a Leidenfrost droplet is offered based on a simplified droplet geometry and employing the assumptions considered in refs. [5–7]. A heat balance at the base of the droplet yields

$$\frac{d\bar{V}}{d\tau} = -\beta\bar{V}^{7/12} \quad (3)$$

where

$$\beta = \left(\frac{\Delta T^3 V_0}{12B} \right)^{1/4} \frac{\xi \rho_g C_p}{L_m \rho_l} \quad (4)$$

$$B = \frac{1}{8} \left[\frac{3f_2^{3/2}}{4\pi f_1} \right]^{4/3} \frac{\pi k_g \mu_g}{L_m \rho_g g} \quad (5)$$

$$\xi = \left(\frac{3\pi^{1/2} f_2^{3/2}}{4 f_1} \right)^{2/3} \quad (6)$$

and

$$L_m = L_1 \varepsilon_1 + L_2 \varepsilon_2. \quad (7)$$

Integrating equation (3) from $\bar{V} = 1$ yields

$$\bar{V} = [1 - \beta\tau]^{12/5}. \quad (8)$$

Both components will evaporate from the emulsion at their fractional evaporation rates ε_i according to the evolution law expressed by equation (8) until one of the components is depleted. At this time the droplet volume \bar{V} , is given by a mass balance as

$$\bar{V}_i = 1 - \frac{\rho_i \Phi_i}{\rho_l \varepsilon_i} \quad (9)$$

and $i = 1$ or 2 . The value of i is determined by the larger of \bar{V}_1 or \bar{V}_2 . From the time of depletion of one of the components to complete evaporation ($\bar{V} = 0$), equation (3) can be integrated to yield

$$\bar{V} = [\bar{V}_i - \beta_i(\tau - \tau_i)]^{12/5} \quad (10)$$

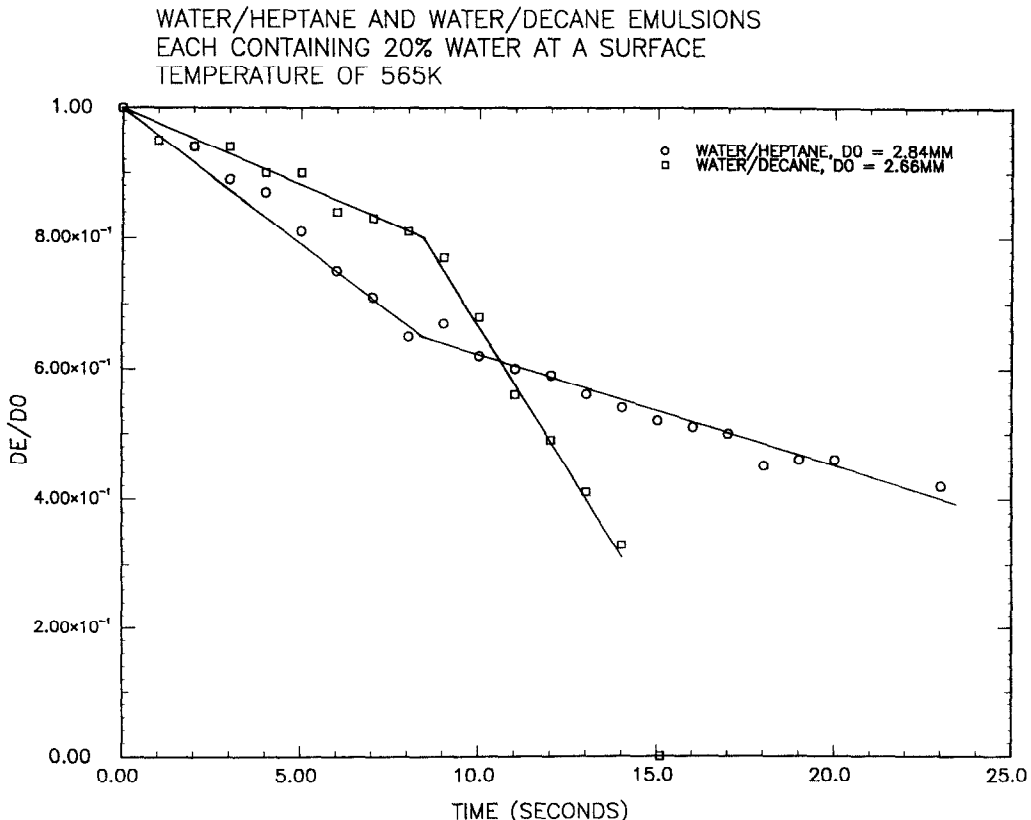


Fig. 9. Evolution of a 20% water/heptane and a 20% water/decane emulsion droplet at $T_p = 565$ K. Preferential evaporation is signified by the 'knee' in the variation.

where β_i is given by equations (4) and (5) with all properties pertaining to component i , and

$$\tau_i = \frac{1 - \bar{V}_i^{5/12}}{\beta} \quad (11)$$

Here ε_i is obtained from the simplest model which leads to preferential evaporation of the emulsion components. In such a model the emulsion components are considered to vaporize independently of their liquid phase concentration. In this so-called 'distillation limit' [13] the equilibrium vaporization temperature of the emulsion is given by

$$P_0 = P_{1e}(T_s) + P_{2e}(T_s) \quad (12)$$

where $P_0 = 0.101$ MPa in the present work. At the base of the droplet, the evaporation rate per unit area of each component is approximated by

$$m_i = h_m(\rho_{is} - \rho_{ib}) \quad (13)$$

where h_m is the mass transfer coefficient. For simplicity, it will be assumed that h_m is a constant. Then with

$$\varepsilon_i = \frac{m_i}{m} \quad (14)$$

and

$$m = \sum_i m_i \quad (15)$$

equations (9)–(11) yield

$$\varepsilon_i = \frac{\rho_{is} - \rho_{ib}}{\rho_s - \rho_b} \quad (16)$$

By defining a non-dimensionalized density in the vapor film as

$$\phi = \frac{\rho_{is} - \rho_i}{\rho_{is} - \rho_{ib}} \quad (17)$$

the bulk vapor density can be obtained by evaluating ϕ at the heated surface ($\phi = \phi_w$):

$$\rho_{ib} = \frac{\rho_{is}(\phi_w - 1) + \rho_{iw}}{\phi_w} \quad (18)$$

where ρ_{is} is evaluated at the droplet temperature ($= \rho_i(T_s)$) and $\rho_{iw} = \rho_i(T_p)$.

To evaluate ϕ_w the detailed concentration field of the vapor beneath the droplet must be determined by solving the governing species conservation equation. A very simple model for this problem is described in the Appendix. It is shown that $\phi_w \approx 1.394$. With ε_i known the evolution of the droplet diameter can be obtained.

To illustrate, a 50% water-in-heptane emulsion is considered with a solid surface temperature of 620 K. All pertinent properties for water and heptane were obtained from refs. [17, 18]. For a total gas pressure beneath the droplet of about 0.101 MPa, the maximum steady-state temperature of the emulsion

droplet as determined from equation (8) is about 351 K. All bulk component gas properties were evaluated at an average temperature between the surface and droplet, and mixture properties were estimated based on a gas phase mole fraction average of the component properties. Mixture densities were obtained by summing the component densities. The properties used to evaluate β in equation (8) were average gas phase values, except for L_m which was weighted by the fractional evaporation rate. Figure 10 illustrates the evolution of normalized droplet diameter for water, heptane, and a 50% water-in-heptane emulsion. Calculations for two values of ε_i are shown: one obtained from equation (16) and one obtained by arbitrarily setting $\varepsilon_i = 0.5$. The *qualitative* trends for the evolution of diameter of water and heptane which are predicted from equations (8) to (10) conform with the experimental results of Figs. 2–8. The evolution of diameter for the emulsion exhibits a discontinuity when one of the emulsion components is completely depleted from the droplet. The subsequent evolution of diameter is controlled by the component that remains. The reason for this depletion is that the emulsion components will evaporate in the order of their relative volatilities, so that one of the components will be evaporating faster. In the early period of evaporation both components participate in the evaporation process and the evolution of diameter is intermediate between that of either component alone.

Whether or not water or the particular hydrocarbon in question evaporates first depends on the value of ε_i . As shown in Fig. 10, for a fractional mass evaporation rate of water calculated from equation (16) (which for the properties used is $\varepsilon_1 \approx 0.99$) water evaporates first. For a lower ε_i (which, for illustration was chosen as $\varepsilon_1 = 0.5$) heptane is predicted to evaporate first. Our experimental results clearly show that heptane is depleted from the droplet first whereas decane appears to evaporate first in a water/decane emulsion (cf. Fig. 9). Thus while the above model does not quantitatively predict the data, the mechanism for preferential evaporation is revealed for an emulsified liquid droplet in Leidenfrost evaporation, namely a distillation-type of evaporation.

If the emulsion components dissolve during evaporation, evaporation could still take place in the order of the relative volatilities of the constituent components. Such preferential evaporation could also lead to a period in which only one component is left inside the droplet. The behavior shown in Fig. 10 would then still be observed.

Variations of the equivalent droplet diameter occasionally revealed peculiar behavior for several of the emulsions tested: the measured effective diameter appeared to *increase* as shown, for example, by the data marked with an arrow in Fig. 2. During this period the droplets also tended to vibrate. The problem stems from the fact that when viewed from one direction only, vibrating droplets are probably not

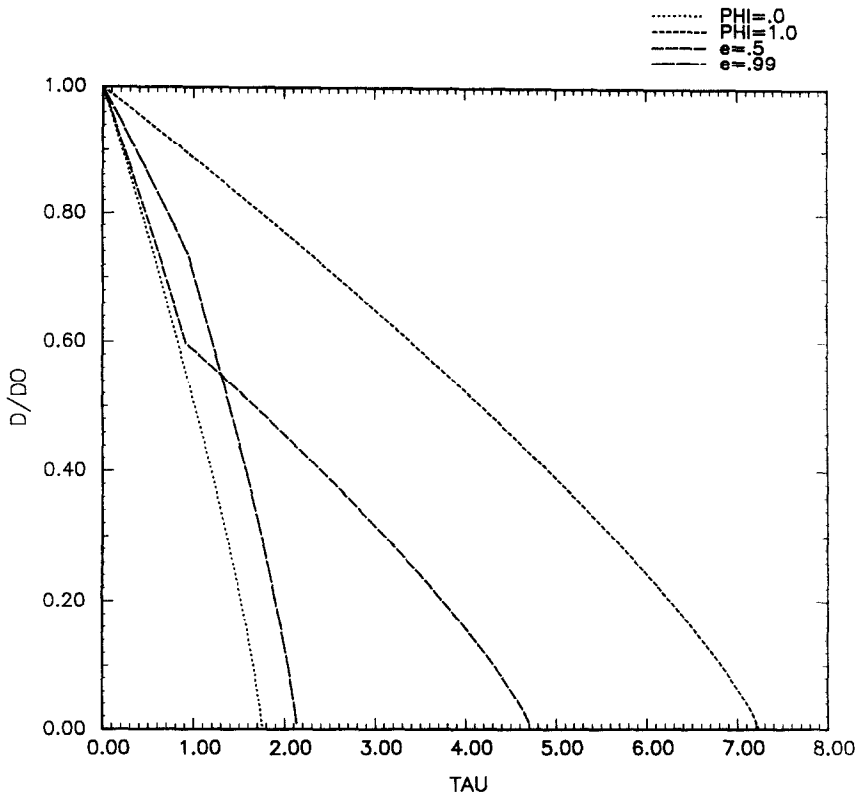


FIG. 10. Predicted evolution of droplet diameter of water, heptane and a 50% water/heptane emulsion at two values of ϵ_1 : 0.5 and 0.99.

axisymmetric, and therefore would not be volumes of revolution. At any instant, it is quite possible that the effective area, when measured in one direction, could be different from the area measured by viewing in another direction. This behavior also seems to have been an artifact of some of the measurements reported by Tamura and Tanasawa [9] for several pure normal alkane droplets. At later times when vibrations cease, the droplets more closely resemble volumes of revolution and the equivalent diameter monotonically decreases.

Figure 11 illustrates the variation of total evaporation time (corresponding to $d_c = 0$ in Figs. 2–8) with the initial volume fraction of water for water/decane emulsions over the range $\Phi \leq 0.5$. Emulsions containing more than 50% by volume of water were not stable. The lines are curves of best fit to illustrate the variation. At a constant surface temperature, the total evaporation time increases as the initial concentration of water in the emulsion increases. This increased evaporation time of an emulsion reveals a perhaps negative characteristic of using emulsified liquids as fuels: water/hydrocarbon emulsions which do not undergo micro-explosions may be prone to incomplete combustion due to this potential increase in evaporation time. The micro-explosion phenomenon could compensate through the creation of smaller droplets.

3.2. Qualitative characteristics of evaporation

Several of the initially 'milky' colored emulsion droplets became 'clear' during evaporation. Figures 12–15 show photographic evidence of this effect for emulsions of water with octane, nonane, decane and dodecane, respectively, at a surface temperature of 565 K and an initial water concentration of 20%. The photographs were taken using direct front lighting with a framing rate of 1 frame s^{-1} . Such clearing was also reported by Law *et al.* [13] in some preliminary Leidenfrost experiments.

Clearing may be due to one or more of the following:

- (1) dissolution of water into fuel;
- (2) coalescence of internal water micro-droplets;
- (3) preferential vaporization of one of the emulsion components.

Dissolving of superheated water droplets into several normal alkanes was previously observed at high temperatures (> 470 K) [19]. When an initially clear water/hydrocarbon mixture was cooled, a 'cloudy' mixture was produced. This suggested that if the temperature of the droplet/hydrocarbon system attained a so-called 'critical solution temperature' (CST) water would dissolve into the hydrocarbon. For temperatures below the CST two phases coexist and water comes out of the mixture as fine droplets. Such

VARIATION OF EVAPORATION TIME FOR DECANE/WATER EMULSIONS AS A FUNCTION OF INITIAL VOLUME FRACTION OF WATER AND SURFACE TEMPERATURE.

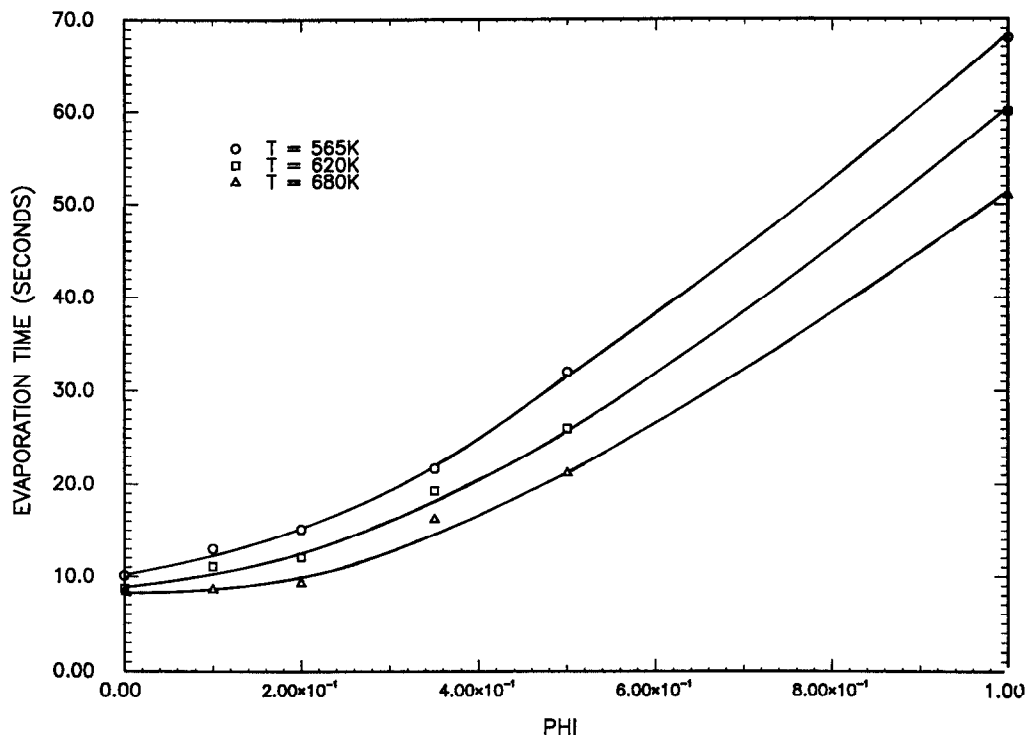


FIG. 11. Variation of total evaporation time with initial volume fraction of water for a water/decane emulsion at $T_p = 565, 620$ and 680 K.

coexistence for emulsions is characterized by a milky or cloudy color.

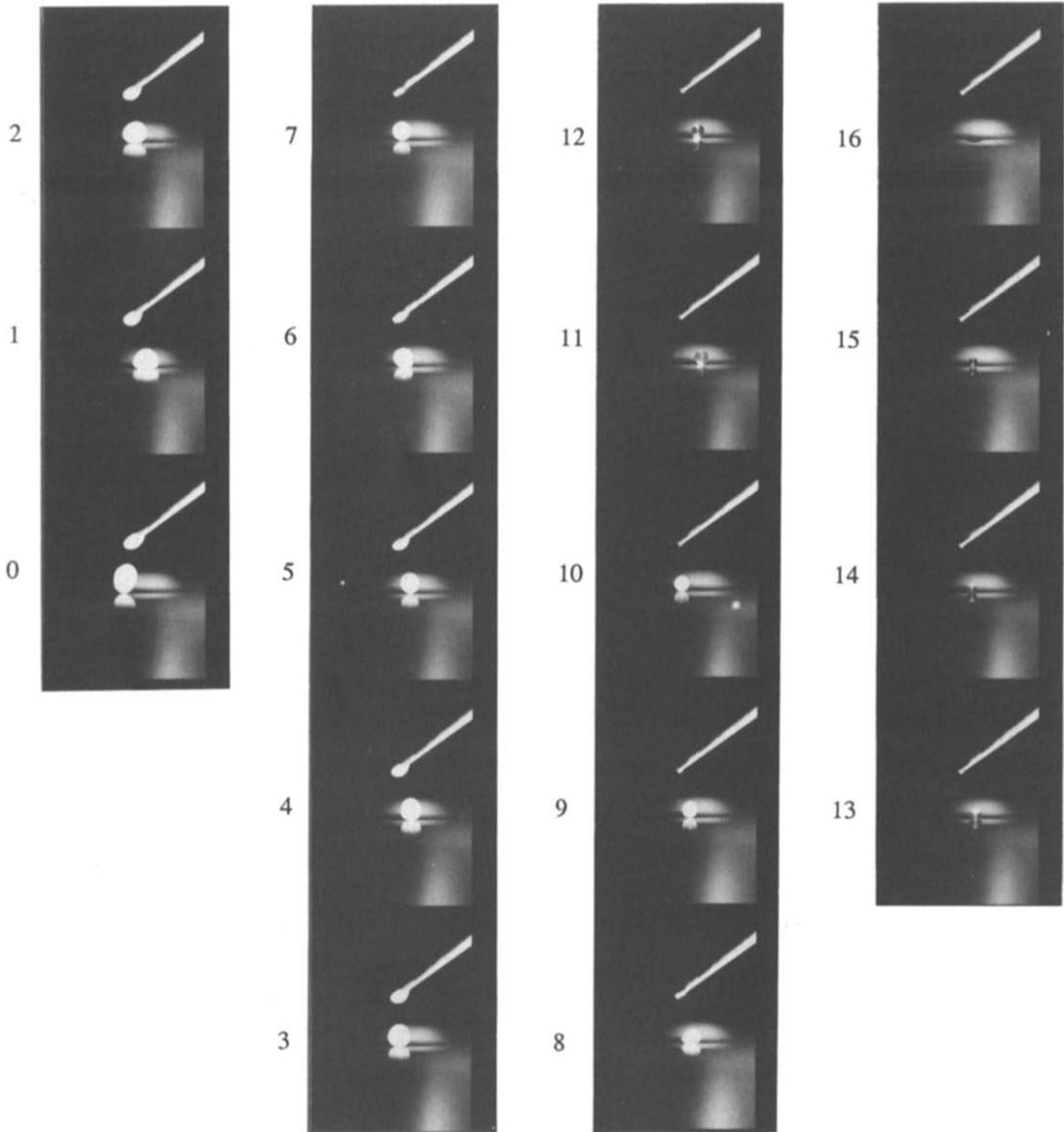
A 'local' clearing such as illustrated in frame 12 of Fig. 14 was also observed. It could have been indicative of temperature gradients within the droplet in regions of the droplet where the temperature is below the CST the cloudiness (i.e. milky color) persists, whereas in regions where the temperature is above the CST the mixture is clear (frames 10–13 of Fig. 14). Though the CST is typically quite high for water/n-alkane systems [19], its value could be reduced in the presence of a surfactant.

Coalescence of internal water micro-droplets apparently also occurred, as a single lump of internal phase was observed at various times during evaporation (e.g. see frames 8 and 10 of Fig. 15 for a water/dodecane emulsion). This coalescence apparently leads to a phase separation and partial clearing of a droplet as for example shown in Fig. 12 (frames 11 and 13) and Fig. 15 (frame 8). The image of the light bulbs used for direct front lighting is reflected in several of the photographs, for example in frame 7 of Fig. 13, and should not be misunderstood as coalesced water droplets.

The preferential vaporization mechanism discussed previously could promote clearing of an emulsion droplet only when water prevaporizes before the

hydrocarbon: a mixture of the hydrocarbon and surfactants used here was transparent whereas a water/surfactant mixture had a milky color. If the hydrocarbon is preferentially depleted from the droplet first (as in the water/heptane emulsion) the remaining mixture of water and surfactants could then still maintain its initial milky appearance even in the absence of fuel (unless the CST of the water/surfactant mixture is exceeded, such as at the end of evaporation). Thus, preferential vaporization may not be responsible for clearing of the water/decane emulsions because water apparently preferentially evaporates first for that emulsion (cf. Figs. 2–4).

During evaporation internal movement of liquid was occasionally observed in a partially transparent emulsion droplet and the droplets sometimes oscillated. Frames 6–15 of Fig. 15 are indicative of the observed oscillations for emulsions as manifested by their changing shape with time. Oscillatory movement undoubtedly contributed to the difficulties previously noted in interpreting the droplet diameter measurements since the droplets were only observed in one direction. Internal circulatory motion of liquid was frequently observed by the movement of particles inside the droplet, which were apparently picked up by the evaporating droplet from the surface. In such cases, the photographic data were rejected.



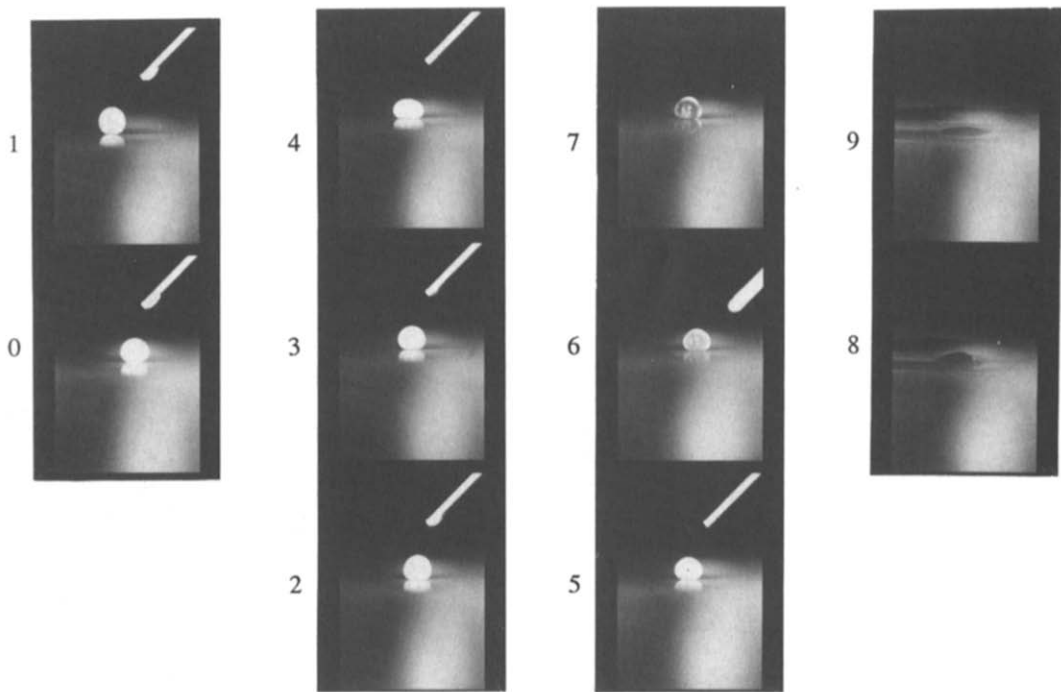
Water/Octane

$\Phi = 0.20$

$T_p = 565\text{K}, T_\infty = 296\text{K}$

$V_0 = 12$ microliters, Framing rate = 1 sec, Front lighting

FIG. 12. Photographic sequence of an evaporating 20% water/octane droplet at $T_p = 565\text{K}$. Front lighting is used to illustrate clearing of the droplet during evaporation (frames 10–15). Framing rate is 1 frame s^{-1} .



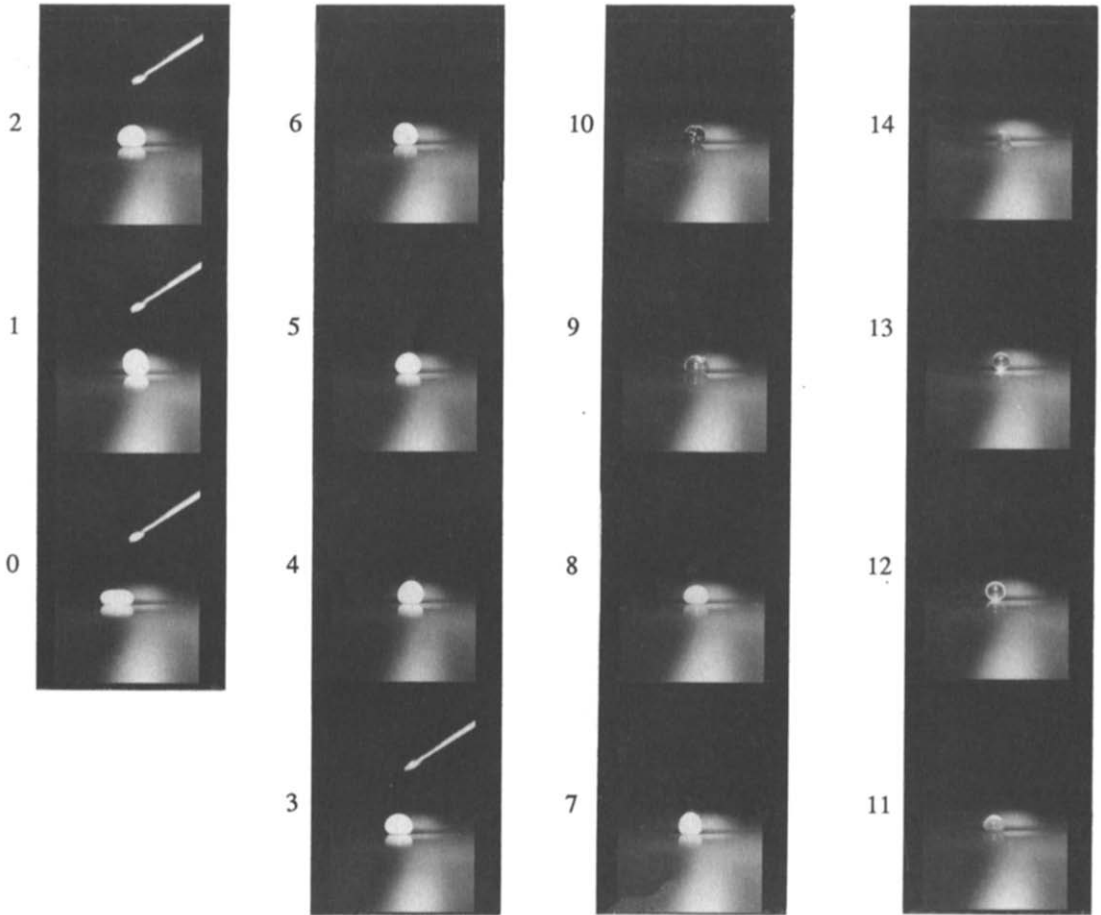
Water/Nonane

$$\Phi = 0.20$$

$$T_p = 565\text{K}, T_\infty = 296\text{K}$$

$V_0 = 12$ microliters, Framing rate = 1 sec, Front lighting

FIG. 13. Photographic sequence of a 20% water/nonane droplet at $T_p = 565$ K. Partial clearing of droplet is shown in frames 5–7.



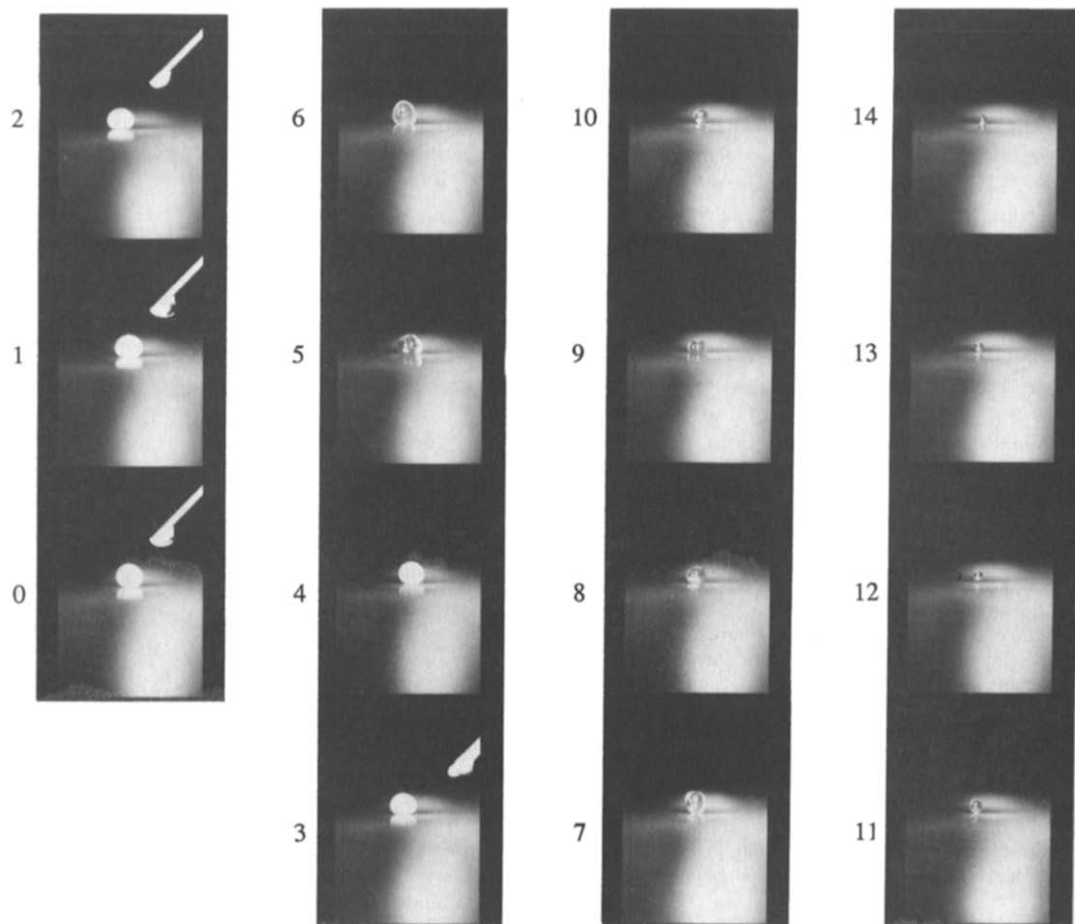
Water/Decane

$$\Phi = 0.20$$

$$T_p = 565\text{K}, T_\infty = 296\text{K}$$

$V_0 = 12$ microliters, Framing rate = 1 sec, Front lighting

FIG. 14. Photographic sequence of a 20% water/decane droplet at $T_p = 565$ K. A cyclic clearing is shown in frames 8–14.



Water/Dodecane

$$\Phi = 0.20$$

$$T_p = 565K, T_\infty = 296K$$

$V_0 = 12$ microliters, Framing rate = 1 sec, Front lighting

FIG. 15.

4. CONCLUSIONS

Preferential vaporization of either fuel or water can occur from an evaporating water-in-fuel emulsion droplet. For heptane/water emulsions, heptane was preferentially evaporated from the droplets, whereas for water/decane emulsions, water prevaporized before decane. This effect was thought to be indicative of a change in the evaporation constant of the droplets, shifting toward that of water or fuel during evaporation. The initial volume concentration of water apparently had a minimal effect (within the range studied) on whether water or fuel would be preferentially vaporized from the droplet. The emulsions appeared to clear up during their evaporation. This effect was believed to be caused either by the dissolution of water into fuel or coalescence of internal water micro-droplets.

Acknowledgements—This work formed part of a project supported by DOE contract No. DE-AC02-83ER13092. Additional support was received from NSF grant No. CBT-8451075. The authors are indebted to Dr W. R. C. Phillips for helpful discussions.

REFERENCES

1. E. C. Owens and B. R. Wright, Engine performance and fire-safety characteristics of water-containing diesel fuels, AFLRL Report No. 83, U.S. Army Fuels and Lubricants Research Laboratory, Southwest Research Institute, San Antonio, Texas, December (1976).
2. F. L. Dryer, Water addition to practical combustion systems—concepts and applications, 16th Symp. (Int.) Combust., pp. 279–295 (1976).
3. J. R. Nicholls, I. A. El-Messiri and H. K. Newhall, Inlet manifold water injection for control of nitrogen oxide—theory and experiment, SAE paper No. 690018, January (1969).
4. K. J. Baumeister and F. F. Simon, Leidenfrost temperature—its correlation for liquid metals, cryogenics, hydrocarbons and water, *J. Heat Transfer* **95**, 166–173 (1973).
5. K. J. Bell, The Leidenfrost phenomenon: a survey, *Chem. Engng Prog. Symp. Ser.* **63**(79), 73–82 (1967).
6. C. T. Avedisian, C. Ioffredo and M. J. O'Connor, Film boiling of discrete droplets of mixtures of coal and water on a horizontal brass surface, *Chem. Engng Sci.* **39**, 319–327 (1984).
7. C. T. Avedisian and J. Koplik, Leidenfrost boiling of methanol droplets on hot porous/ceramic surfaces, *Int. J. Heat Mass Transfer* **30**, 379–393 (1987).
8. G. S. Emmerson, The effect of pressure and surface materials on the Leidenfrost point of discrete drops of water, *Int. J. Heat Mass Transfer* **18**, 381–386 (1975).
9. Z. Tamura and Z. Tanasawa, Evaporation and combustion of a drop contacting with a hot surface, 7th Symp. (Int.) Combust., pp. 509–522 (1959).
10. K. Makino and K. Michiyoshi, The behavior of a water droplet on a heated surface, *Int. J. Heat Mass Transfer* **27**, 781–791 (1984).
11. S. Sheffield, M. R. Baer and C. J. Denison, Paper Nos. 42 and 43, Fall Technical Meeting, Eastern States Section of the Combustion Institute, Princeton, New Jersey (1980).
12. P. Cho, M.S. Thesis, Northwestern University (1981).
13. C. K. Law, C. H. Lee and N. Srinivasan, Combustion characteristics of water-in-oil emulsion droplets, *Combust. Flame* **37**, 125–143 (1980).
14. C. H. Wang, Ph.D. Thesis, Northwestern University (1983).
15. S. Satcunanathan, Evaporation rates of liquid droplets in the spheroidal state on a hot surface, *J. Mech. Engng Sci.* **10**, 438–441 (1968).
16. M. Seaver, Naval Research Laboratory, Private communication (21 July 1987).
17. J. H. Keenan, F. G. Keyes, P. G. Hill and J. G. Moore, *Steam Tables*. Wiley, New York (1969).
18. K. E. Starling, *Fluid Thermodynamic Properties for Light Petroleum Systems*. Gulf, Houston, Texas (1973).
19. C. T. Avedisian and I. Glassman, Superheating and boiling of water in hydrocarbons at high pressures, *Int. J. Heat Mass Transfer* **24**, 695–706 (1981).
20. W. R. C. Phillips, Private communication (May 1987).
21. R. K. Shah and A. L. London, *Laminar Flow Forced Convection in Ducts*, p. 158. Academic Press, New York (1978).

APPENDIX

Vapor outgassing beneath a Leidenfrost droplet is assumed to resemble fully developed laminar flow between parallel plates as modelled in Fig. A1. The governing species conservation equation can be written in the following form:

$$\frac{d^2\phi}{dy^2} = -Sh v_x \phi \quad (\text{A1})$$

where

$$v_x = 3/2(1 - 4y^2) \quad (\text{A2})$$

$-1/2 \leq y \leq 1/2$ and Sh is the Sherwood number. The boundary conditions are

$$y = 1/2 \begin{cases} \phi = 0 \\ \frac{d\phi}{dy} = -Sh \end{cases} \quad (\text{A3})$$

and

$$y = -1/2, \quad \frac{d\phi}{dy} = 0. \quad (\text{A5})$$

Equation (A5) is the condition of impermeability of the surface.

The solution to equations (A1) and (A2) is [20]

$$\phi = e^{-2\lambda^2 y^2} [C_1 F_1 + C_2 \lambda^{1/2} y F_2] \quad (\text{A6})$$

where F_1 and F_2 are the hypergeometric functions

$$F_1 = M((1-\lambda)/4, 1/2, 4\lambda y^2) \quad (\text{A7})$$

$$F_2 = M((3-\lambda)/4, 3/2, 4\lambda y^2) \quad (\text{A8})$$

and

$$\lambda = \left(\frac{3}{8} Sh \right)^{1/2} \quad (\text{A9})$$

C_1 , C_2 and λ are determined from equations (A3)–(A5)

$$C_1 = \frac{-\frac{8}{3} \lambda^2 e^{4/2}}{\frac{dF_1}{dy} \Big|_{y=1/2} - \frac{F_1(1/2)}{F_2(1/2)} \frac{dF_2}{dy} \Big|_{y=1/2} - 2F_1(1/2)} \quad (\text{A10})$$

$$C_2 = C_1 \frac{F_1(1/2)}{\lambda^{1/2} F_2(1/2)} \quad (\text{A11})$$

while λ is obtained from the solution to

$$\frac{dF_1}{dy} \Big|_{y=-1/2} - 2 \frac{F_1(-1/2)}{F_2(-1/2)} \left[F_2(-1/2) - 1/2 \frac{dF_2}{dy} \Big|_{y=-1/2} \right] + 4\lambda F_1(-1/2) = 0. \quad (\text{A12})$$

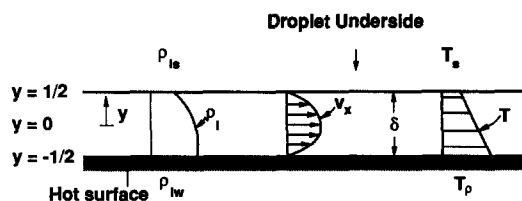


Fig. A1. Model of vapor flow underneath a Leidenfrost droplet.

There are an infinite number of λ which satisfy equation (A12), but only the lowest positive value gives a physically meaningful concentration profile. The correct solution is $\lambda \approx 0.95467$, which yields $Sh \approx 2.43039$ (which is also identical to the value of the Nusselt number corresponding to fully developed laminar flow between parallel plates with one plate insulated and the other plate maintained at a constant temperature [21]). Equations (A6)–(A11) evaluated at $y = -1/2$ (the hot surface) gives $\phi(-1/2) = \phi_w = 1.394019$, which could be used to obtain a bulk vapor density from equation (18).

ETUDE EXPERIMENTALE DES CARACTERISTIQUES DE L'EVAPORATION DU TYPE LEIDENFROST DE GOUTTELETTES LIQUIDES EMULSIFIEES

Résumé—On décrit des observations expérimentales sur les caractéristiques de l'évaporation de gouttelettes d'émulsion d'eau dans du fioul sur une surface horizontale chaude. Des mesures détaillées de la variation temporelle du diamètre équivalent de goutte pour des émulsions d'eau–heptane et eau–décane sont faites pour des températures de surface 565, 620 et 680 K. Les expériences sont conduites à la pression atmosphérique avec des concentrations d'eau de 10, 20, 35 et 50%. D'autres caractéristiques sont observées pour des émulsions d'eau avec octane, nonane et dodécane. On trouve que les émulsions eau–heptane et eau–décane montrent une vaporisation préférentielle telle que l'eau ou l'hydrocarbure s'évapore en premier (respectivement pour les émulsions de decane et d'heptane). Ce résultat est révélé par une discontinuité apparente dans l'évolution du diamètre équivalent de goutte et il est expliqué à partir d'un modèle de distillation pour l'évaporation. Des résultats montrent aussi que la vitesse d'évaporation diminue et que le temps d'évaporation totale augmente avec un accroissement du contenu d'eau. Les gouttelettes initialement opaques deviennent plus claires pendant la vaporisation pour plusieurs des émulsions considérées. On observe aussi la coalescence de la phase interne pour les émulsions eau–octane et eau–dodécane. Parmi les couples essayés, seul eau–heptane montre une caractéristique disruptive à la fin du mécanisme d'évaporation.

EXPERIMENTELLE UNTERSUCHUNG DER LEIDENFROST-VERDAMPFUNG VON EMULSIONSTROPFEN

Zusammenfassung—Experimentelle Beobachtungen beim Filmsieden von in Kraftstoff emulgierten Wassertropfen auf einer horizontalen Fläche werden vorgestellt. Es wurden umfangreiche Messungen der zeitlichen Änderung des gleichwertigen Tropfendurchmessers von Wasser–Heptan- und Wasser–Dekan-Emulsionen bei Oberflächen-Temperaturen von 565, 620 und 680 K durchgeführt. Die Versuche erfolgten bei Atmosphärendruck und volumetrischen Anfangskonzentrationen des Wassers von 10, 20, 35 und 50%. Weitere qualitative Eigenschaften von Emulsionen von Wasser in Oktan, Nonan und Dodekan wurden beobachtet. Es wurde festgestellt, daß Wasser–Heptan- und Wasser–Dekan-Emulsionen eine vorzugsweise Verdampfung zeigten, derart, daß entweder das Wasser oder der Kohlenwasserstoff zuerst verdampfte (für Dekan- bzw. Heptan-Emulsionen). Dieses Ergebnis zeigte sich durch eine offensichtliche Unstetigkeit in der Entwicklung des gleichwertigen Tropfendurchmessers und wird auf der Basis eines einfachen Destillations-Grenzen-Modells für Verdampfung erklärt. Die Ergebnisse zeigen weiterhin, daß mit steigendem Wassergehalt die Tropfen-Verdampfungsgeschwindigkeit sinkt und die Gesamtverdampfungszeit zunimmt. Die anfänglich trüben Tropfen wurden bei einigen der untersuchten Emulsionen während der Verdampfung klar. Ebenso wurde das Zusammenwachsen der emulgiert Phase bei Wasser–Oktan- und Wasser–Dodekan-Emulsionen beobachtet. Von den untersuchten Emulsionen zeigten nur die Wasser–Heptan-Emulsionen Spaltungserscheinungen zum Ende des Verdampfungsprozesses.

ЭКСПЕРИМЕНТАЛЬНОЕ ИЗУЧЕНИЕ ХАРАКТЕРИСТИК ИСПАРЕНИЯ КАПЕЛЬ ЭМУЛЬГИРОВАННОЙ ЖИДКОСТИ В РЕЖИМЕ ЛЕЙДЕНФРОСТА

Аннотация—Представлены результаты экспериментального исследования характеристик испарения капель водо–топливной эмульсии при пленочном кипении на горячей горизонтальной поверхности. Подробные измерения изменений во времени эквивалентного диаметра капли эмульсий воды в декане и воды в гептане были проведены при температурах поверхности 565, 620 и 680 К. Эксперименты проводились при атмосферном давлении; изучались начальные объемные концентрации воды в 10, 20, 35 и 50%-эмульсиях. Для эмульсии воды в октане, нонане и додекане наблюдалось больше качественных характеристик. В эмульсиях вода/гептан и вода/декан обнаружено избирательное испарение, т.е. либо вода, либо углеводород испарялись в первую очередь (соответственно, для эмульсий декана или гептана). Этот результат был обнаружен из-за прерывного характера изменения эквивалентного диаметра капли и объясняется на основе простой предельной модели перегонки для испарения. Результаты показывают также, что скорость испарения капли уменьшается, и общее время испарения капли возрастает с увеличением содержания воды. При испарении некоторых исследуемых эмульсий, наблюдалось обесцвечивание первоначально непрозрачных цветных капель, а также слияние внутренней фазы для эмульсий вода/октан, вода/додекан. Из всех изученных эмульсий только для эмульсии вода/гептан не получена разрывная характеристика в конце процесса испарения.